Bioresource Technology 440 (2026) 133404

Contents lists available at ScienceDirect

Bioresource Technology

journal homepage: www.elsevier.com/locate/biortech

Thermochemical conversion of oil palm empty fruit bunch into fuel gas in a fluidized bed gasifier

Amanda Assunção Rosa Silva [a,b], Gabriel Ferreira da Silva Brito [a], Thainá Araruna [a], Rossano Gambetta [b], Fabricio Machado [a,*]

[a] Instituto de Química, Universidade de Brasília, Campus Universitário Darcy Ribeiro, CEP, Brasília 70910-900 DF, Brazil
[b] Embrapa Agroenergia, Parque Estação Biológica, PqEB s/n, W3 Norte, CEP, Brasília 70770-901 DF, Brazil

HIGHLIGHTS

- Oil palm empty fruit bunch (OPEFB) was successfully converted into fuel gases.
- Pilot-scale gasification was carried out with three gasifiers in a fluidized reactor.
- OPEFB has a high volatile content and a favorable composition for fuel formation.
- Steam gasification yielded the highest H_2 (52 % v/v) and CH_4 (0.05 g/g biomass).
- Gasifying agent defines the syngas composition: air raises CO, steam boosts H_2/CH_4.

GRAPHICAL ABSTRACT

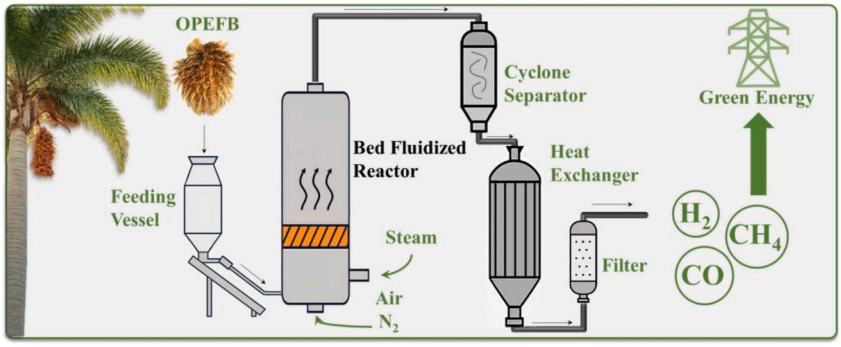

ARTICLE INFO

Keywords:
Oil palm empty fruit bunches (OPEFB)
Biomass conversion
Thermochemical conversion
Green energy

ABSTRACT

With increasing energy demand and agro-industrial waste generation, sustainable solutions for biomass valorization become essential. This study investigates the thermochemical conversion of oil palm empty fruit bunches (OPEFB) in a pilot-scale fluidized bed gasifier using air, steam, and nitrogen as gasifying agents. OPEFB characterization confirmed its favorable composition for energy purposes, including high volatile matter and lignocellulosic content. Gasification experiments revealed that the choice of gasifying agent strongly influenced syngas composition and yield. Air gasification maximized CO production, reaching 0.56 g/g biomass at an equivalence ratio (ER) of 0.43. Steam gasification produced the highest hydrogen and methane yields, with up to 52 % v/v H_2 and 0.05 g CH_4/g biomass, which are comparable to, or even higher than, those reported elsewhere for other lignocellulosic biomasses under similar conditions. Nitrogen atmosphere suppressed oxidation and promoted moderate H_2 formation. These findings demonstrate that steam is the most effective agent for hydrogen-rich syngas generation, while air favors CO production. Overall, the study highlights OPEFB as a

Abbreviations: ASE, Accelerated Solvent Extractor; CHN, Carbon, Hydrogen and Nitrogen; DME, Dimethyl Ether; ER, Equivalence Ratio; FC, Fixed Carbon; HHV, High Heating Value; HPLC, High Pressure Liquid Chromatography; LHV, Low Heating Value; OPEFB, Oil Palm Empty Fruit Bunches; Rgb, Produced Gas to Fed Biomass Ratio; RID, Refractive Index Detector; Rsb, Steam-to-biomass Ratios; SAF, Sustaintable Aviation Fuels; Syngas, Synthesis Gas; TG/DTA, Thermogravimetric Analysis /Differential Thermal Analysis; XRF/EDX, X-Ray Fluorescence Spectrometer.

* Corresponding author.
E-mail address: fmachado@unb.br (F. Machado).

https://doi.org/10.1016/j.biortech.2025.133404
Received 9 June 2025; Received in revised form 27 August 2025; Accepted 26 September 2025
Available online 27 September 2025

promising feedstock for clean energy and biorefinery applications, supporting the transition toward a circular and sustainable bioeconomy.

1. Introduction

Currently, most of the primary energy consumed worldwide originates from fossil fuels. Due to climate change, the pursuit of energy security, and growing environmental awareness, efforts are being made to diversify the energy matrix with renewable and sustainable sources such as solar, wind, geothermal, tidal, and biomass (Gayen et al., 2023; Strielkowski et al., 2021). Biomass stands out as an attractive renewable energy option, ranking among the largest energy sources globally and offering advantages such as lowering greenhouse gas emissions and contributing to socioeconomic and environmentally sustainable development (Al Zubi et al., 2023; Ang et al., 2022; Méndez-Durazno et al., 2024; Mignogna et al., 2024; Razm et al., 2023; Sarker et al., 2015; Yana et al., 2022). Unlike petroleum, biomass is widely available across countries, and its use can diversify the fuel supplies and enhance energy security, particularly for nations reliant on oil imports (Bilgili et al., 2017; Fernandes and Costa, 2010).

Palm oil is one of the most consumed oils worldwide, and it is estimated that for every ton of palm oil produced, approximately 1.1 tons of oil palm empty fruit bunches (OPEFB) are generated (Hossain et al., 2016). This residue, which often becomes an environmental problem, holds significant potential for energy applications and the production of high-value products, including biofuels, making it a promising feedstock for biorefineries (Chuaboon et al., 2024; Hendrasetiafitri et al., 2022; Obada et al., 2023; Tanimu et al., 2025). OPEFB is not only abundant but also has a lignocellulosic nature. Its composition, consisting of approximately 50.9 % cellulose, 29.6 % hemicellulose, and 17.8 % lignin, is comparable to that of other agricultural residues extensively studied for energy applications, such as sugarcane bagasse and corn stover (Kumar and Sharma, 2017; Padzil et al., 2020). Given these features, we hypothesize that OPEFB has significant potential as a feedstock for thermochemical conversion.

Biomass can be converted into three main products: fuel for the transportation sector, fuel for the generation of heat and power, and raw material for the synthesis of high value-added chemical products (Jamil et al., 2024; Maitlo et al., 2022). Among the processes available to carry out such conversions, biomass gasification has gained interest due to its high conversion efficiency and broad applications. Traditionally, coal has been widely used as the primary feedstock for gasification (Gao et al., 2023; Sansaniwal et al., 2017). Lignocellulosic biomass, however, emerges as more sustainable alternative, presenting high fixed carbon content, low ash and sulfur levels, and potential for carbon neutrality, in addition to being derived largely from agricultural residues. Its composition favors both the release of combustible volatiles and the generation of higher energy–density products, which reinforces its viability as a substitute for coal in thermochemical processes (Cherwoo et al., 2023; Santana et al., 2025; Shahzad et al., 2024). In this context, OPEFB stands out for its suitability as a lignocellulosic feedstock, coupling favorable composition with large-scale generation in palm oil production, positioning itself as one of the most promising residues for gasification and bioenergy generation (Asadpour et al., 2021; Nyakuma et al., 2020; Singh et al., 2025). Recent research in major palm oil-producing countries has focused on valorizing OPEFB through thermochemical routes. Al-Muraisy et al. (2025) investigated solar-driven CO_2 gasification of OPEFB, demonstrating the production of CO-rich synthesis gas (syngas) with high carbon conversion efficiency (94.9 %) and simultaneous biochar generation, highlighting its potential as a negative-emission technology and sustainable energy pathway. Ahmad et al. (2023) explored the use of OPEFB gasification char, activated by phosphoric acid, as a low-cost adsorbent for wastewater treatment, reporting efficient removal of methylene blue dye and confirming the value of gasification by-products beyond energy applications. These studies underscore the versatility of OPEFB in gasification routes.

The gaseous product obtained from the thermochemical process of gasification, known as syngas, consists mainly of a mixture of H_2, CO, CO_2, H_2O, N_2, and other light hydrocarbons. Syngas is produced by partial oxidation of organic material at elevated temperatures and can either be combusted for energy generation or used as precursor for the synthesis of higher-value chemical products, such as methanol, dimethyl ether (DME), and liquid fuels obtained through Fischer-Tropsch process (Santos and Alencer, 2020). Interest in syngas valorization routes has grown, with particular emphasis on the production of green hydrogen, renewable methanol, and sustainable aviation fuels (SAF), aligning with global strategies for energy transition and decarbonization (Hidalgo et al., 2025; Ismael et al., 2025; Klüh et al., 2024; Mustafa et al., 2024). Gasification involves drying and devolatilization (pyrolysis) of biomass, during which large amounts of volatile hydrocarbons and char are produced and subsequently are converted into syngas.

In this regard, the accumulation of volatiles significantly influences the reaction rate, and reactor design is critical for enhancing the gasification process (Gao et al., 2023; Sher et al., 2025). Fluidized bed gasifiers, in particular, offer key advantages such as increasing the contact surface between bed material and biomass particles and promoting temperature homogenization, which improves the reaction rate and overall conversion efficiency. These benefits arise from the simultaneous occurrence of pyrolysis and gasification stages within the reactor, preventing the buildup of volatile compounds (Gómez-Barea and Leckner, 2010; Lahijani and Zainal, 2011). Furthermore, fluidized bed gasification technology can operate under various and with a wide range of feedstocks, and its performance is strongly influenced by factors such as fuel type, particle size, reaction temperature, reactor configuration, gasifying agent, and equivalence ratio (ER) (David, 2013; Pfeifer et al., 2011; Santos et al., 2022). Recent studies have highlighted the potential of the fluidized bed to enhance process efficiency. Miccio et al. (2021) presented the advantages of fluidized-bed systems over fixed bed, moving bed, and rotary-kiln systems for the gasification of agricultural wastes, emphasizing improvements in mass and heat transfer efficiency. Siddiqui et al. (2022) developed studies on the gasification of various biomasses in fluidized bed reactors, focusing on enhancing biomass conversion and syngas production efficiency by optimizing operating parameters such as particle size and catalyst use. The use of impregnated catalysts significantly boosted H_2 and syngas yields, improved the water–gas shift reaction, and reduced CO_2 and tar formation.

In the field of lignocellulosic biomass, gasification in fluidized bed reactors has proven to be a promising route for clean energy production. Figueroa et al. (2014) studied the effects of varying the ER and temperature during sugarcane gasification on the production and distribution of syngas, bio-tar, and char. The study showed that higher ER levels increased hydrogen and carbon monoxide production, while CO_2 emissions decreased, demonstrating the flexibility of fluidized bed systems. Furthermore, the bio-tar yield was mainly water, highlighting the potential of such systems to produce cleaner energy from biomass residues. Another work by Pedroso et al. (2021) focused on the roasting of sugarcane bagasse to optimize its use as a biofuel feedstock, addressing challenges associated with its fibrous nature and high moisture content by optimizing roasting conditions. The study reported improvements in energy yield and reductions in pollutant emissions.

Nevertheless, most studies in the literature have focused on conventional lignocellulosic feedstocks in fluidized bed configurations, while systematic investigations on OPEFB are still limited, highlighting the need for further research on this underutilized residue, since OPEFB

has similar lignocellulosic characteristics and is equally viable for this type of process (Kurnia et al., 2016; Umar et al., 2021). So far, only a few studies have addressed the gasification of OPEFB in fluidized bed reactors. Sukiran et al. (2009) studied OPEFB pyrolysis in a quartz fluidized-fixed bed reactor, optimizing parameters such as temperature, particle size, and heating rate, and achieving a maximum bio-oil yield of 42 % at 500 °C, confirming the relevance of fluidized systems for maximizing liquid fuel production from this residue. Lahijani and Zainal (2011) explored OPEFB gasification in a pilot-scale bubbling fluidized bed, finding that temperatures up to 1050 °C improved carbon conversion (93 %) and cold gas efficiency (72 %), but also induced severe bed agglomeration due to the high potassium and chlorine content of the ash, which they mitigated by lowering the operating temperature to 770 °C. More recently, Sidek et al. (2021) compared raw and torrefied OPEFB in a steam fluidized bed gasifier, showing that torrefaction enhanced syngas yield, lower heating value, and cold gas efficiency, although it also increased tar generation, highlighting the trade-off between energy output and downstream cleaning requirements. Despite these contributions, the current literature on OPEFB remains scarce, with key gaps still to be addressed: (i) the lack of systematic studies on OPEFB gasification, (ii) the limited number of investigations employing OPEFB specifically in fluidized bed reactors, and (iii) the absence of comparative analyses assessing the influence of different gasifying agents on process efficiency and product distribution. Addressing these issues is essential to unlock the full potential of OPEFB as a sustainable feedstock for fluidized bed gasification.

In light of these limitations and to the best of our knowledge, this is the first work to conduct a comparative experimental analysis of OPEFB gasification in a fluidized bed reactor under three gasifying atmospheres (air, water vapor, and N_2). The study provides detailed insights into the effects of these agents on the production of key gaseous components (H_2, CO, and CH_4), highlighting the role of water vapor in enhancing hydrogen generation. By coupling physicochemical characterization of OPEFB with performance evaluation against a conventional lignocellulosic feedstock (sugarcane bagasse), this research not only advances the technical understanding of OPEFB gasification but also demonstrates its potential as a sustainable alternative for clean energy generation. Ultimately, the study contributes to closing the loop in the palm oil production chain, transforming a major agro-industrial residue into a valuable resource for renewable energy and circular-bioeconomy applications.

2. Materials and methods

This section describes the materials and methodologies adopted to evaluate the thermochemical conversion of OPEFB into fuel gases under various conditions. The steps include biomass preparation, physicochemical characterization, and thermochemical tests in a fluidized bed reactor. Each step was designed to gather relevant data for understanding the influence of gasifying agents on gas composition and process performance.

2.1. Sample preparation

The OPEFB used in this study were obtained from Belém, Brazil. The dry OPEFB was ground using a Willey Macro knife mill (Fortinox, STAR FT-60) to obtain a particle size distribution in the range of 0.30 to 0.85 mm by using a set of sieves (Bronzinox, São Paulo, Brazil) with the following mesh sizes: 10, 20, 50, 100, 200, and 500.

2.2. Biomass characterization

2.2.1. Proximate analysis

The moisture, volatile matter, ashes and fixed carbon (FC) contents were determined in triplicate according to ASTM D 5142-02a standard (Vassilev et al., 2012) using a LECO TGA 701 thermogravimetric analyzer.

For the moisture determination, the samples weighed in previously tared porcelain crucibles were heated in the equipment at 107 °C in N_2 atmosphere to constant weight.

After the determination of humidity, the volatile matter was determined as follows. The crucibles were capped and weighed in the equipment. The equipment was then heated to 950 °C under N_2 at a rate of 50 °C min^{-1} and held for 7 min at this temperature.

Ashes content was determined after the determination of the volatile matter; the furnace of the equipment was cooled from 950 °C to 600 °C and the atmosphere changed from N_2 to O_2. The temperature was then raised to 750 °C and samples were weighed at regular intervals to constant mass. The FC percentage was calculated by subtracting the percentages of moisture, ashes and volatile matter (see the Supplementary Material).

2.2.2. Elementary analysis

Carbon, hydrogen, and nitrogen (CHN) were determined using a PerkinElmer CHNS/O analyzer (model 2400 Series II), operated at 925 °C (combustion column) and 650 °C (reduction column), using helium as the carrier gas and oxygen as the oxidizing gas. Two to three milligrams of finely ground and oven-dried sample (105 °C, constant weight) were used. The amount of oxygen by difference was obtained with the ash content and the percentages of carbon, hydrogen and nitrogen.

Additionally, X-ray fluorescence spectrometer (XRF / EDX) of the Shimadzu brand, model EDX 720 HS, was used to analyze some elements from the 3rd period of the periodic table present in the samples, in vacuum with a 5 mm collimator and a beam ranging from 50 keV (Sc-Ti channel, 0.02 step) to 15 keV (Na-Sc channel, 0.01 step) with 2048 points. This equipment allows the analysis of the range of elements covering from sodium (^{11}Na) to uranium (^{92}U).

2.2.3. Extractives

The extractives content of the biomass was determined following the Extractives Content Determination protocol described by NREL (NREL/TP-510–42619) (Cortez et al., 2008) with modifications using an Accelerated Solvent Extractor (ASE) (Thermo Scientific Dionex ASE-350). Glass fiber filter was used at the base of each cell, filling it with the sample up to its maximum capacity without compacting the sample. Extraction was carried out using an ethanol (≥99 %, Sigma-Aldrich), petroleum ether (boiling range 40–60 °C, Merck) solution (1:2) through three 30 min cycles at 105 °C. Extract-free samples were removed from the cells, transferred to a tray, and allowed to air-dry at room temperature for approximately 24 h. The vials containing the extracts were placed in a rotary evaporator to remove the solvents and the remaining extractives were quantified gravimetrically.

2.2.4. Lignin

Lignin and structural carbohydrate contents were determined on extractive-free biomass, following the NREL protocol (NREL/TP-510–42618) with modifications, in triplicate. Each pressure tube received 0.30 g of extractive-free biomass and 3 mL of 72 % sulfuric acid (analytical grade, Dinâmica Química Contemporânea, Brazil). The tubes were placed in a water bath at 30 °C for 60 min, with manual agitation every 10 min (without removing the tubes from the bath). After one hour, the tubes were removed from the bath, 84 mL of distilled water were added to each one, shaken to homogenize the solution, and then taken to an autoclave at 121 °C for 60 min. Hydrolyzed samples were filtered, under vacuum, in previously tared *Gooch* crucibles (porosity #4). A 50 mL of the liquor was collected in a falcon tube and analyzed, in triplicate, in a UV–Visible spectrophotometer with a wavelength of 240 nm, using a 4 % sulfuric acid solution as blank (Blank Abs). In cases where the sample was too concentrated, it was diluted with the blank solution, and the dilution ratio was recorded.

After the analysis of the liquors, all remaining solids in each tube

were quantitatively transferred to the respective crucibles using at least 50 mL of hot distilled water to remove all acid. The crucibles were placed in an oven at 105 °C overnight. After being removed from the oven, the mass of the crucibles with the residue of insoluble lignin and ashes was recorded.

The crucibles with residue were then placed in a muffle furnace and subjected to five heating stages, as described in Table 1.

After cooling down to temperatures below 200 °C, the crucibles were removed from the muffle furnace and transferred to an oven at 105 °C for 2 h. After being removed from the oven, the crucibles were weighed on an analytical balance and the mass of the crucible with the ash residue was recorded.

The soluble lignin content, based on extractive-free material (% Lignin), was determined using the volume of the liquor and the absorptivity equivalent to 25 L $g^{-1}cm^{-1}$, used to determine the absorbances of the liquor and the blank. More details can be seen in the Supplementary Material.

The insoluble lignin content, based on extractive-free material (% InsLignin), was determined based on the difference of the overnight oven crucible weight and muffle furnace crucible weight (see the Supplementary Material).

2.2.5. Carbohydrates

Liquor from the lignin determination step was filtered using a 0.22 μm syringe filter, then transferred to a glass vial and analyzed in a Shimadzu HPLC (High Pressure Liquid Chromatography), using an Aminex HPX-87P column with pre-column and refractive index detector (RID). Volume of injection of 10 μL and ultrapure water (Milli-Q system) was the mobile phase at a flow rate of 0.6 mL min^{-1}. The run lasted 32 min, with the column and detector temperatures fixed at 85 °C.

The mass value, in grams, of each compound was calculated multiplying the total volume of the solution, expressed in liters, and the concentration of the compound obtained at the end of the HPLC analysis (see the Supplementary Material).

Monomeric sugar concentrations were converted to masses using equation described in the Supplementary Material. Polymeric sugars were calculated using the following conversion factors (see Supplementary Material): glucose to glucan, 0.90 (or 162/180); xylose to xylan and arabinose to arabinan, 0.88 (or 132/150); and acetic acid to acetate, 0.983 (or 59/60).

The percentages of structural carbohydrates and acetyl groups were calculated from the relationship between the corrected mass obtained in the calculation of the mass of polymeric sugars and the sample weight (Supplementary Material). Results are expressed on a dry basis of the raw material.

2.2.6. High heating value and low heating value

High Heating Value (HHV) were obtained using an IKA calorimeter model C-2000, according to ASTM D 5865-04 (Saidur et al., 2011). Low Heating Value (LHV) was calculated according to the literature (Cortez et al., 2008).

2.2.7. Thermal analyzes

The TG/DTA (thermogravimetric analysis) curves were obtained in a Simultaneous DTA-TG Thermogravimetric Analyzer (Shimadzu, DTG-60H) with nitrogen purge (30 mL·min^{-1}). The analyzes heated from room temperature to 900 °C at a heating rate of 10 °C·min^{-1} in platinum crucibles.

Table 1
Heating stages associated with the temperatures used during the thermal treatment for lignin and ash analysis of oil palm empty fruit bunches.

Stage	Initial temperature (°C)	Final temperature (°C)	Time (min)
1	0	100	15
2	100	300	25
3	300	300	30
4	300	500	25
5	500	500	180

2.2.8. Particle size distribution

Particle size distribution was determined using a Bertel sieve shaker with a Bronzinox sieves (ISO 3310/1), with mesh sizes: 10, 20, 50, 100, 200, 500.

2.3. Pilot plant for gasification and pyrolysis

Thermochemical conversion tests were performed in a PID Eng and Tech pilot-scale gasification and pyrolysis unit (Scheme 1 and figures in the Supplementary Material), capable of operating with air, steam, oxygen, and CO_2 as gasifying agents, or nitrogen under pyrolysis conditions. Gases were fed through mass flow controllers and preheated (300–400 °C) before reaching the reactor. Water was pumped, evaporated, and introduced as steam. Solids were stored in a silo and fed using dual screw feeders to prevent premature reaction.

A fluidized bed reactor (see Supplementary Material) with silica bed (1.00 kg, mesh 30, d_{max} = 0.30 mm) was used. The reactor has a total height of 1515 mm, comprising a bed zone (770 mm in length and 82.8 mm in internal diameter) and a freeboard zone (535 mm in height and 134.5 mm in internal diameter). Temperatures were monitored by thermocouples (three in the bed, one in the freeboard), and pressures by transducers (one before the distributor plate and another at the top of the freeboard). The reactor was heated to 800 °C and the operating pressure drop ranged from 16 to 20 mBar. Once stabilized, ~400 g of biomass was fed at flowrates in the interval between 0.86 and 6.09 g·min^{-1}. The ER applied in air gasification ranged from 0.29 to 0.43, depending on the air flow rates used (8–12 NL·min^{-1}). For steam gasification, the R_{sb} were in the range from 1.75 to 2.19, corresponding to steam flowrates of 12 and 15 mL·min^{-1}, respectively. Under nitrogen atmosphere, flow rates of 12, 15, and 18 NL·min^{-1} were employed. Generated gas passed through two cyclones to remove particulates, then through a heat exchanger (18–30 °C) for tar condensation, and finally through a particulate filter.

2.4. Gas analyzer

The gases generated during the gasification process were analyzed using an inline gas analyzer from SICK, model GMS800. This analyzer has four different modules responsible for determining the concentrations of H_2, O_2, H_2S, CO, CO_2, and CH_4. Each gas was calibrated using a standard mixture with a known concentration.

3. Results and discussion

The results are structured to first assess the physicochemical properties of the biomass, which are essential to evaluate its suitability for gasification. Subsequently, the performance of the gasification process under different operating conditions and gasifying agents is analyzed. The aim is to identify how these variables influence the composition and yield of syngas, with particular attention to the generation of key gases such as H_2, CO, and CH_4.

3.1. Proximate analysis

To ensure the viability of biomass use in a fluidized bed gasifier, the moisture content must remain below 10 %, as high moisture levels hinder solid feeding, reduce gasification efficiency, and lower the calorific value of the final gas (Molino et al., 2016). As observed in the data of Table 2, OPEFB had a desirable moisture value for the process. A high ash content also contributes to reducing the calorific value of the gas produced, as ash is inert and does not contribute to gas production during gasification. Therefore, materials with low ash content are more

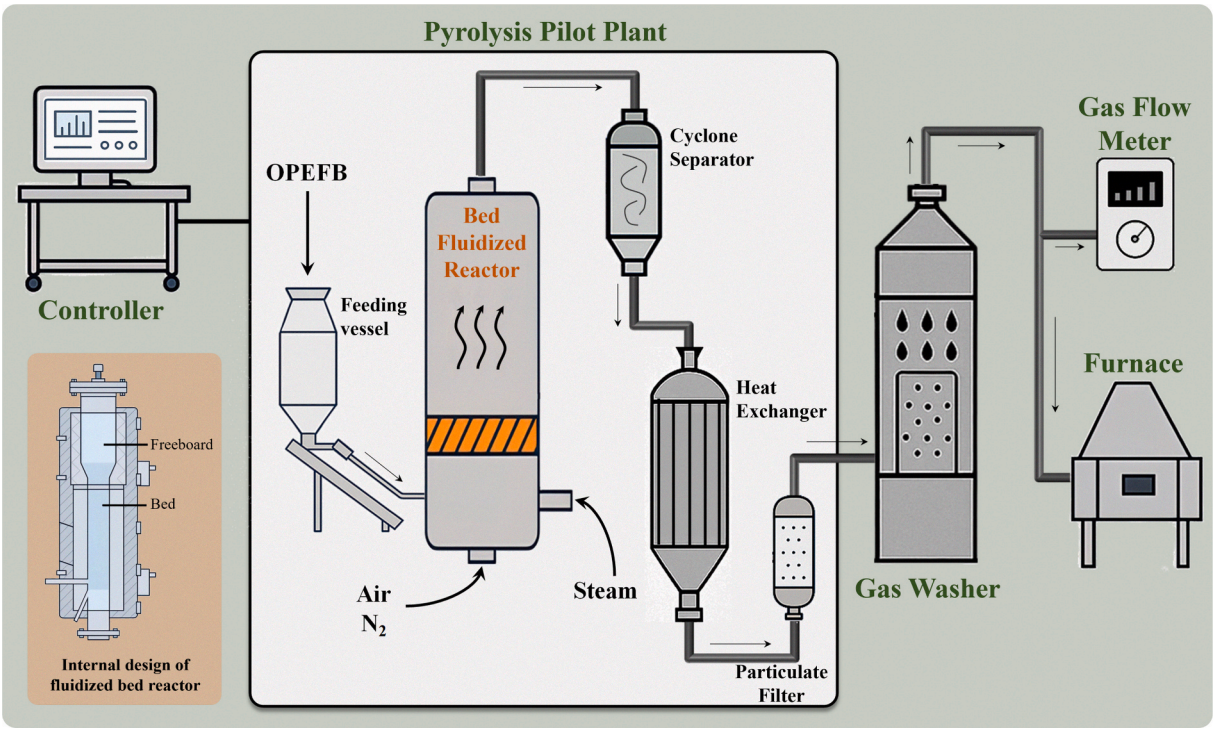

Scheme 1. Schematic diagram of the gasification and pyrolysis pilot plant.

Table 2
Characterization oil palm empty fruit bunches to provide information on their proximate, ultimate inorganic and lignocellulosic composition.

Proximate analysis (%)										
Humidity (%)	Volatile matter (%)			Fixed Carbon (%)					Ashes (%)	
6.18 ± 0.01	72.62 ± 0.27			15.93 ± 0.41					5.27 ± 0.22	
Elemental analysis (CHN/O) on dry basis (%)										
Carbon	Hydrogen			Nitrogen		Sulfur			Oxygen	
45.16 ± 0.50	6.09 ± 0.09			1.35 ± 0.02		1.43			40.70	
Inorganic materials (%)										
K	Ca	Si	P	Mg	S	Fe	Zn	Mn	Cu	Sr
59.187	26.034	4.660	2.266	1.397	1.426	3.089	1.193	0.455	0.207	0.086
Composition of fractionated lignocellulosic (%)										
Ashes	Extractives		Lignin		Cellulose		Hemicellulose		Mass Closure	
6.53 ± 0.25	8.55 ± 0.09		41.29 ± 0.25		28.91 ± 0.19		20.73 ± 0.80		106.01 ± 1.58	

appropriate for thermochemical processes, causing less fouling, deposition, agglomeration, and corrosion problems (Vassilev et al., 2015). Compared with some residual biomasses, the OPEFB has a high ash content, but is still much lower than other biomasses such as rice husk (21.24 %), cotton stem (17.30 %) and avian bed (37.80 %) (Saidur et al., 2011).

Comparing the values obtained on dry basis to other biomasses such as bark and rice straw, wheat straw and even some types of wood (Kalinci et al., 2011), the volatile content of OPEFB is higher. Higher volatile contents result in lower ignition temperatures, as well as making ignition, devolatilization and burning processes easier and faster and increase the production of combustible gas and inorganic vapors (Vassilev et al., 2015).

According to Vassilev et al. (2015), volatile biomass materials consist mainly of fuel species such as: CH_4, C_2H_2, CO, H_2, H_2S, tar and other hydrocarbons, especially light ones; besides non-combustible components, such as: CO_2, HCl, H_2O, N_2, NH_3, NO_x (NO, NO_2), N_2O, KCl, KOH, NaCl, NaOH, SO_x (SO_2, SO_3), among others. It is noteworthy that due to high volatile contents, biofuels present a high reactivity when compared to coal (Khan et al., 2009).

3.2. Ultimate analysis: CHNO elemental analysis

Based on the values of carbon (C), hydrogen (H), and nitrogen (N) obtained from the elemental analysis, as well as the sulfur (S) content measured by XRF/EDX and the ash content from the proximate analysis, the oxygen (O) content was estimated by difference, i.e., by subtracting the sum of these components from 100 %. The results of the elemental analysis for OPEFB biomass are presented in Table 2. The oxygen content observed for the OPEFB is average, while the carbon content is lower than average reported for most of the biomasses, which typically contain around 50 %. Both the low carbon content and the high oxygen content result in a decrease in the calorific value of the generated gas. According to Jenkins et al. (1998), each additional 1 % of carbon in the biomass composition increases the calorific value by about 0.39 $MJ{\cdot}kg^{-1}$.

In addition, the CHNO contents will also have direct consequences on the composition of the gas, since these elements are precursors to the main gaseous products in the thermochemical processes: H_2, CO, CO_2, NO_x, CH_4 and other light hydrocarbons. High hydrogen contents in the composition of the biomass, for instance, favors the increase of H_2 and CH_4 production, which in turn enhances the energy content of the resulting gas.

3.3. X-ray fluorescence by dispersive energy (XRF/EDX)

According to Khan et al. (2009), ashes can be defined as the non-combustible inorganic part of the biomass remaining after the process, containing the mineral fraction of the original biomass. The characterization of the inorganic materials is particularly relevant for the OPEFB, which has a relatively high ash content. In this case, the high potassium content as shown in Table 2 directly influences the gasification process, since the presence of this metal decreases the melting point of the ash, causing bed agglomeration and deposit formation on the reactor walls, which can ultimately interfere with the stability of the fluidized bed (Mohammed et al., 2011). Like potassium, silicon, when in high concentration, also reduces ash melting temperature, leading to the aforementioned operational issues. In contrast, elements such as calcium and magnesium tend to increase ash melting temperature, thereby helping to mitigate such effects (Khan et al., 2009).

Ash sintering and melting behavior can vary significantly among biomass types. Understanding these characteristics is essential to determine temperature control, as inadequate control can lead to ash fusion and the formation of deposits along reactor surfaces (Khan et al., 2009).

Although further studies are required regarding the ash behavior and the consequences of its melting during the thermochemical processes, it has been found that the removal of alkaline and other elements makes it possible to increase the melting temperature of the ashes. Recent experiments with sugarcane bagasse showed that the leaching of alkali metals and chlorine by simple washing of the material with water resulted in drastic improvements in the melting temperatures of the ashes. This technique is capable of removing about 80 % of alkali metals and may be a viable strategy to optimize the process (Jenkins et al., 1998).

3.4. Fractionation of lignocellulosic biomasses

Cellulose, hemicellulose and lignin are macromolecules with distinct compositions and structures, which lead to different behaviors during thermal conversion. Therefore, the contents of extractives, lignin, cellulose and hemicellulose in the biomass used were quantified and are shown in Table 2.

In a study carried out by Vassilev et al. (2012), standardized extractive, lignin, cellulose and hemicellulose were reported for 93 varieties of biomasses on an ash-free dry basis. The average composition found was: 43.3 % cellulose, 31.8 % hemicellulose, 24.9 % lignin and 9.5 % extractives. Compared to these values, the OPEFB biomass analyzed in this study exhibited a significantly lower cellulose content and a higher lignin content. These factors have a direct consequence on the calorific value of the sample, as lignin has a lower degree of oxidation compared to cellulose and hemicellulose, thus contributing more to the energy content (Saidur et al., 2011).

The extractive content of OPEFB was also below the average reported by Vassilev et al. (2012). Biomass extractives consist of various organic and inorganic components that could be extracted individually or sequentially using different polar or nonpolar solvents. High extractive content in biomass, more common for herbaceous and agricultural fibers or grasses, is an advantage for the production of biodiesel, bioethanol, biomethanol, among other biofuels and biochemicals. However, for thermochemical conversion biomasses with lower extractive contents are generally more suitable (Vassilev et al., 2015).

3.5. Heating value

According to Cortez et al. (2008), the HHV of a fuel is defined as the amount of energy released as heat during the complete combustion of a unit mass of the material. The results of higher calorific value obtained experimentally was 18.3 ± 0.1 MJ kg^{-1}.

The LHV of a given material is calculated by subtracting the energy required to evaporate the moisture present in the biomass and the formation water generated when the hydrogen in the fuel is oxidized (Cortez et al., 2008; Khan et al., 2009). The LHV found for OPEFB was 19,3 MJ·kg^{-1}. It was verified that the results obtained for the OPEFB are consistent with the literature, since LHV were reported in the range of 17.8 to 19.0 MJ kg^{-1}, close to what was found (Kalinci et al., 2011; Kelly-Yong et al., 2007).

3.6. Thermal analyzes

The thermal stability of OPEFB was evaluated by thermogravimetric analysis. The mass loss curves as a function of temperature (TG) and differential thermal analysis (DTA) are shown in Fig. 1.

The thermal degradation of the biomass can be divided into three regions (Lahijani and Zainal, 2011). The initial mass loss in the range of approximately 50 °C to 120 °C can be attributed to the loss of moisture and volatiles. The second mass loss, quite pronounced, that occurs in the range of 229 °C to 314 °C corresponds to the decomposition of hemicellulose and cellulose and is related to the volatile matter present in the biomass. In the third step, the devolatilization process continues in the range of 314 °C to 547 °C, likely due to the degradation of lignin, which decomposes at higher temperatures than cellulose and hemicellulose. Beyond this temperature range, the mass of the samples remained practically constant up to 900 °C, indicating that the primary organic components are fully decomposed. The ash content observed for OPEFB was approximately 6 %.

3.7. Fluidization tests

Fluidization tests were performed to characterize the main flow regimes at both ambient and reaction temperatures, so that the fluidization behavior was established. These tests provided fundamental information regarding the minimum fluidization velocity – i.e. the point at which the packed bed transitions to fluid-like behavior (incipient, slug, bubbling, turbulent, among others). The experimental results are shown in Fig. 2.

Analysis of the fluidization curves for the three agents found that the minimum fluidization velocity (using 1.00 kg of silica ocher mesh 30)

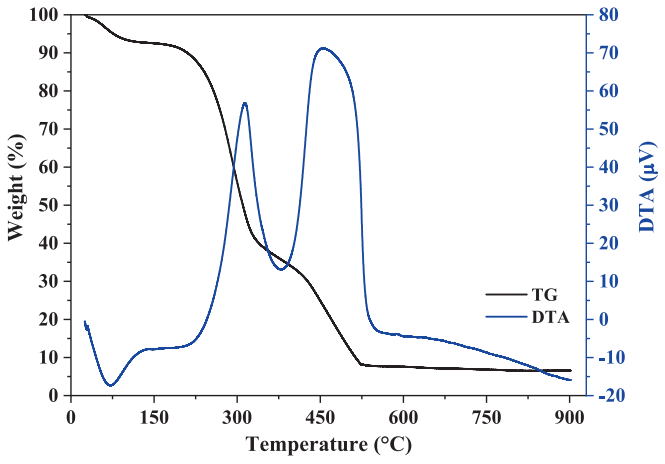

Fig. 1. Thermogravimetric analysis of oil palm empty fruit bunches to evaluate their thermal degradation profile.

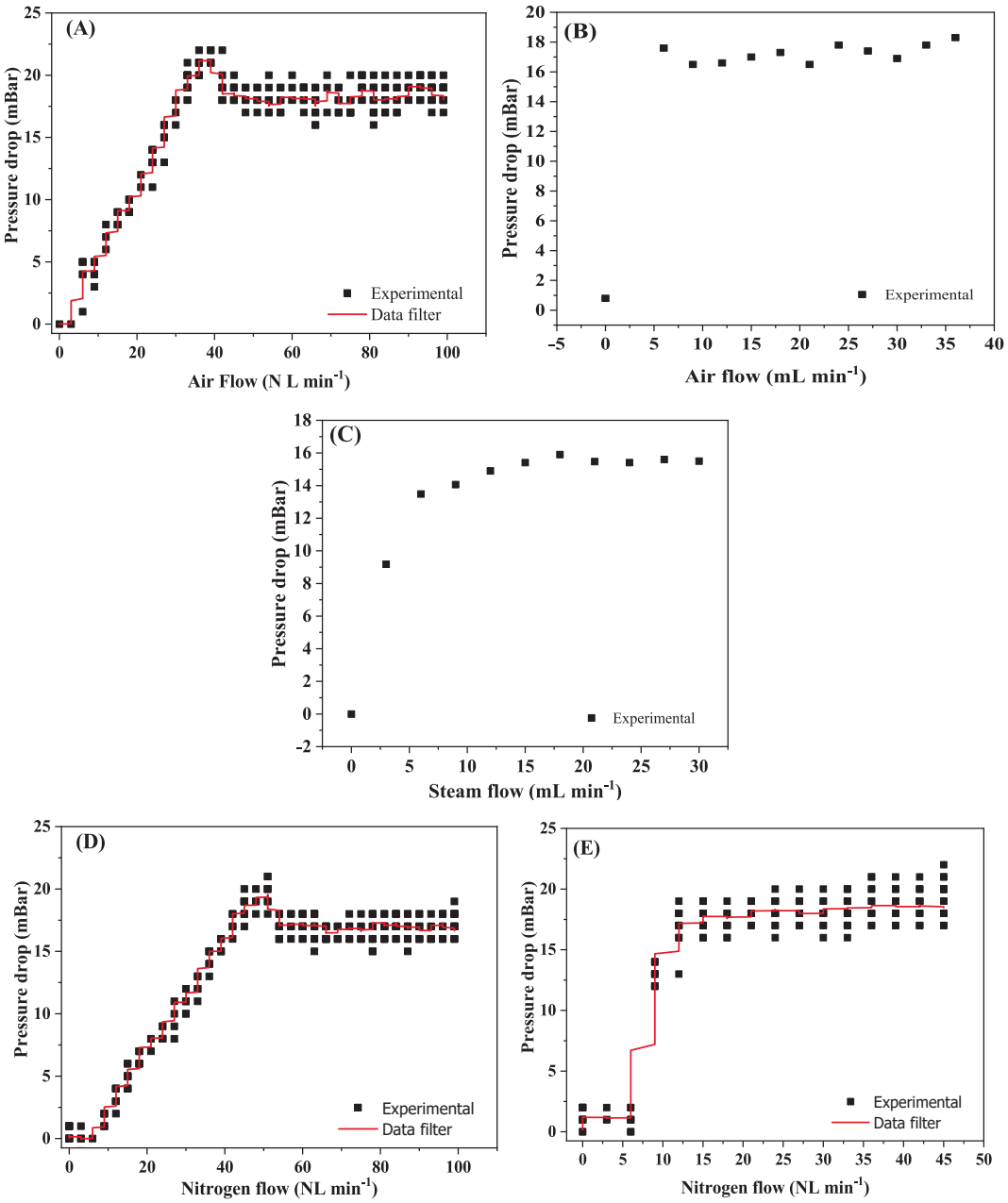

Fig. 2. Profile of the bed load loss as a function of the gas flow: A) air at room temperature; B) air at 800 °C; C) steam at 800 °C; D) nitrogen at room temperature and E) nitrogen at 800 °C.

for air was reached in the range of 35 to 41 NL·min^{-1} at room temperature and from 6 NL·min^{-1} at the 800 °C. For the nitrogen the minimum fluidization velocity was reached in the range of 49 to 52 NL·min^{-1} at room temperature and from 12 NL·min^{-1} at 800 °C. Finally, for the steam the minimum fluidization velocity was verified from 12 mL·min^{-1} at 800 °C.

3.8. Gasification with air

The air flow rates to be used in the process were determined based on the ER, calculated from the average feed rate at 100 % engine speed, as obtained from the calibration curve (Supplementary Material). After each experiment, the actual biomass feed rate was verified, and ER values were adjusted accordingly. It was not possible to use airflows below 8 NL·min^{-1}, due to stability limitations in the mass flow controller.

Considering the minimum fluidization velocity of air at the gasification temperature and the ER range of 0.2 to 0.4, recommended by several authors as ideal for gasification processes (Alauddin et al., 2010; Martínez et al., 2012; Ruiz et al., 2013; Sarker et al., 2015), air-based gasification experiments were performed using flow rates of 8 to 12 NL·min^{-1}. The respective ER of which are shown in Table 3.

Analysis of the gas composition profiles showed that CO and CO_2

Table 3
Equivalence ratios used in gasification with air.

Air Flow (NL·min^{-1})	ER
8	0.29
9	0.32
10	0.36
11	0.40
12	0.43

were the predominant species at all ER values, likely due to partial and complete oxidation of carbon, as represented by Equations 1 and 2, according to Table 4 (Musinguzi et al., 2014).

For ER values of 0.29 and 0.40, a trend was observed in the concentration curves of the CO and H_2, suggesting the predominance of steam gasification reaction (Equation 3, Table 4).

For the condition of ER = 0.43, an opposite behavior was observed in the profiles of CO and CO_2, evidencing that with CO_2 consumption more CO was produced and vice versa. This fact may evidence the occurrence of Boudouard's reaction (Equation 4, Table 4).

Opposite trends in the CO_2 and H_2 profiles, particularly between 240 and 280 min, indicate that the reverse water–gas shift reaction, an endothermic process, may have been favored during that time interval (Equation 5, Table 4).

Maglinao et al. (2015) carried out a study to evaluate the gas produced in the gasification in fluidized bed reactor with three different biomasses: high tonnage sorghum, cotton gin residue and beef cattle manure. They assessed ratios of equivalence ranging from 0.3 to 0.5 and temperatures of 730 to 790 °C. For a fixed temperature of 730 °C and ER = 0.35, a composition of approximately 5 % H_2, 13.5 % CO, 14 % CO_2 and 4 % CH_4, very similar to the composition of gaseous mixture obtained in the present study for gasification of OPEFB for ER = 0.36, where the syngas consisted around 6 % H_2, 13 % CO, 11.5 % CO_2 and 2 % CH_4.

The generation of a gas mixture with high carbon monoxide (CO) content offers substantial potential for a wide range of industrial applications. One possible use is the direct combustion of CO as a fuel for heat and power generation, particularly in boilers and gas turbines. In addition, CO-rich gas serves as a valuable feedstock to produce high value-added chemicals, such as methanol (via the hydrogenation of CO and CO_2), which represents a strategic route due to its potential to yield numerous commercially relevant products widely employed in different industrial sectors (Chan et al., 2021). Another promising pathway is syngas fermentation, in which specific microorganisms convert CO, CO_2, and H_2 into biofuels and various chemicals, including alcohols and organic acids (Pacheco et al., 2023). These two latter applications are particularly attractive, since it is not necessary to clean up the syngas to remove CO_2, once it is used in the process to generate the desired product. Furthermore, the Fischer-Tropsch synthesis constitutes an additional downstream application, involving the hydrogenation of CO to produce long-chain hydrocarbons and oxygenated compounds, enabling the generation of synthetic fuels such as gasoline, kerosene, and diesel (Fu et al., 2025; Santos and Alencer, 2020).

In all cases a rather low H_2S reading was observed, possibly due to its solubility in water (approximately 3370 ppm), which allowed the retention of much of that gas in the gas scrubber. Although H_2S is a combustible gas, its production is undesirable, because when burned it forms sulfur oxides (SO_x), particularly SO_2, a harmful atmospheric pollutant. Moreover, H_2S can poison catalysts used in downstream applications for fuel or chemical synthesis. Gas concentration and mass flow profiles are shown in the Supplementary Material.

Table 4
Main reactions in biomass gasification processes.

Reaction name	Chemical equation	ΔH	Equation number
Partial Combustion	$C(s) + ½O_2(g) \rightleftharpoons CO(g)$	−111 kJ·mol^{-1}	(1)
Complete Combustion	$C(s) + O_2(g) \rightleftharpoons CO_2(g)$	− 394 kJ·mol^{-1}	(2)
Steam Gasification	$C(s) + H_2O(g) \rightleftharpoons CO(g) + H_2(g)$	131 kJ·mol^{-1}	(3)
Boudoard	$C(s) + CO_2(g) \rightleftharpoons 2CO(g)$	173 kJ·mol^{-1}	(4)
Water gas shift reaction	$CO(g) + H_2O(g) \rightleftharpoons CO_2(g) + H_2(g)$	− 41 kJ·mol^{-1}	(5)
Reverse Methanation	$CH_4(g) + H_2O(g) \rightleftharpoons CO(g) + 3H_2(g)$	206 kJ·mol^{-1}	(6)
Reverse Methanation	$CH_4(g) + CO_2(g) \rightleftharpoons 2CO(g) + 2H_2(g)$	247 kJ·mol^{-1}	(7)

3.9. Water steam gasification (or gasification with steam)

The steam flow rates used in the gasification process were chosen according to the fluidization test data and the calculation of the R_{sb}, determined using the average biomass flow rate (at 100 % engine speed) obtained by means of the calibration curve, as shown in Table 5. It is worth mentioning that the steam/biomass ratio is calculated by dividing the flow rate of the steam flow by the biomass feed rate. After the gasification experiments with these steam flows, the mean flow rate of biomass fed during the process (6.84 g·min^{-1}) was verified and the R_{sb} values were corrected.

Preliminary tests using steam as the gasifying agent showed an H_2 production close to and, in some cases, even higher than the maximum detection limit of the in-line gas analyzer (25 % v/v). To avoid inaccurate readings, the produced gas stream was diluted by injecting 15 NL·min^{-1} of nitrogen at the top of the reactor. This dilution ensured accurate measurements without interfering with fluidization.

Fig. 3 shows the gas concentrations (corrected to exclude dilution effects) and the mass flow rates of each major gas produced in steam gasification experiments with R_{sb} values of 1.75 and 2.19.

In the experiments performed with OPEFB using steam as gasification agent, a predominance of H_2 was observed in the concentration of gas produced, with a maximum production of 45 % for R_{sb} = 1.75 and a maximum of 52 % for R_{sb} = 2.19. These values are very interesting, especially when compared to gasification with air, which were in the range of 6 to 8 %. This can be attributed to the fact that most of the H_2-generating reactions involve steam as a reactant, particularly reactions 3, 5, and 6 in Table 4. Similar trends were observed for the three main gases (H_2, CO, and CO_2) at both steam flow rates (12 and 15 mL·min^{-1}), supporting the hypothesis that the above reactions are predominant in the reaction system.

Fremaux et al. (2015) studied the effect of the steam/biomass ratio in the range of 0.5 to 1.0 in gasification processes of wood residues in a fluidized bed gasifier similar to that used in the present study and observed that with the increase of R_{sb}, H_2 production increased, just as it was observed for OPEFB. Kuo et al. (2022) investigated the biomass/waste gasification using a simulated feedstock composed of polyethylene bags, sawdust, and polypropylene particles. They reported H_2 yields up to 38.25 % when employing catalytic bed materials such as activated carbon and zeolite. In contrast, the present study achieved 52 % without any catalyst with a real feedstock. This result highlights the efficiency of the adopted process conditions. Moreover, avoiding catalysts lowers costs, simplifies the process, and enhances sustainability for industrial applications.

The concentration of CH_4 in volumetric percentage in relation to the total volume of gas produced also increased by changing the gaseous agent from air to steam, leaving the range of 1.5–2.5 % for the range of 3–7.5 %. Production of H_2S remained fairly low, close to 2.5 %.

Mechanistically, the introduction of steam provides reactive H_2O that participates in the gasification of char (*e.g.* reaction 3 in Table 4), the water–gas shift reaction (WGS reaction related to reaction 5 in Table 4), and the steam reforming of light hydrocarbons and tars. Most of these pathways are endothermic (reaction 3 and steam reforming), whereas the water–gas shift is exothermic in the forward direction (Mankasem et al., 2024; Mohammad Junaid and Khaled Ali, 2022). At

Table 5
Steam/biomass ratios (R_{sb}) used in steam gasification.

Steam flow (mL·min^{-1})	R_{sb}
12	1.75
15	2.19

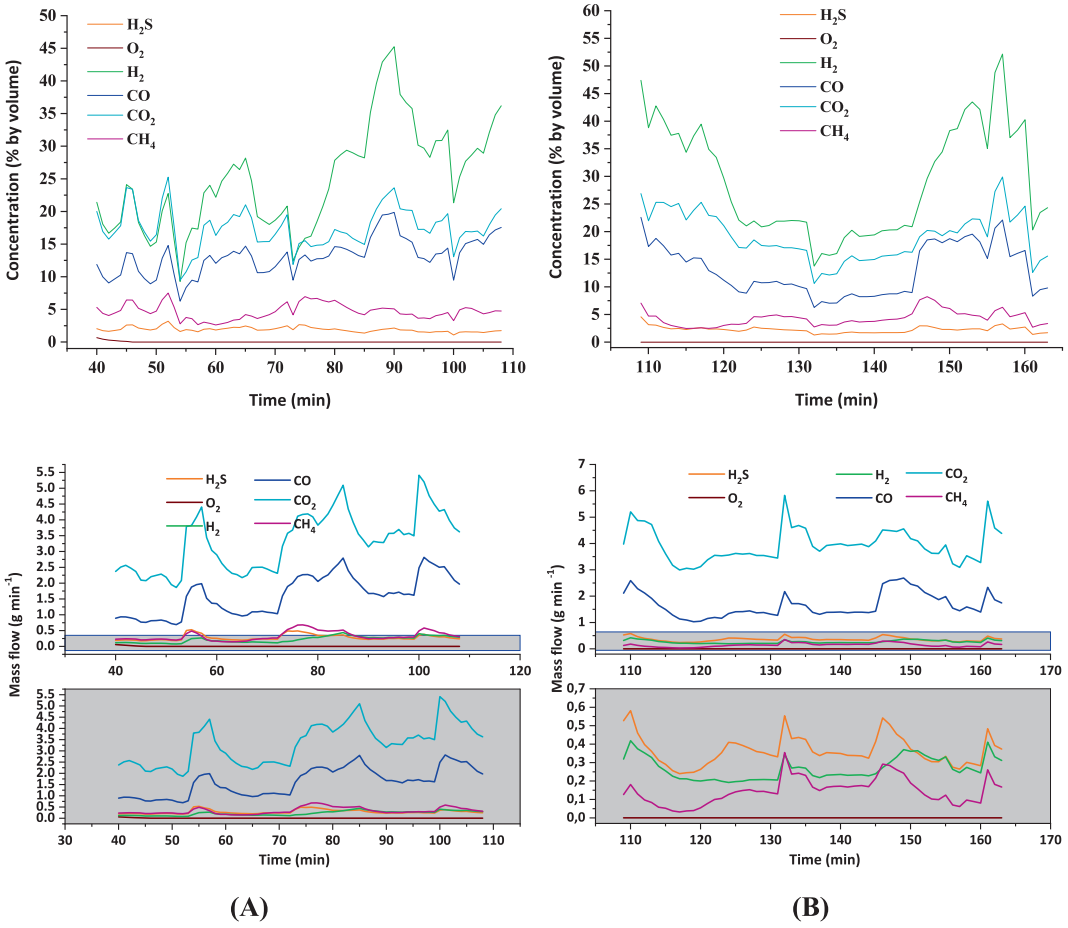

Fig. 3. Concentration and mass flow profiles of process gases with OPFEB for R_{sb} = 1.75 (A) and R_{sb} = 2.19 (B).

~800 °C in the fluidized-bed reactor, the endothermic steps are promoted by heat input and excess steam, while the WGS reaction rapidly equilibrates the gas phase and converts CO to H_2 when favored by local partial pressures. This combined effect explains the observed increase of H_2 under steam. Specifically, WGS enhances H_2 formation by converting CO released during devolatilization and char gasification, while steam reforming of hydrocarbons and tar species provides an additional contribution to hydrogen production (Mankasem et al., 2024; Yang et al., 2019).

Although this latter pathway is often associated with tar reduction under steam-rich atmospheres, the present study focused exclusively on the hydrogen fraction. In relation to CH_4, its main origin is the primary devolatilization during pyrolysis, where light hydrocarbons (including CH_4) begin to appear above ~300–500 °C during biomass heating. This is consistent with pyrolysis gas profiles that show CH_4 emerging at elevated temperatures alongside H_2 (Mankasem et al., 2024). Under air-blown operation, oxidative pathways can consume a portion of these volatiles, while in steam gasification the absence of O_2 removes such sinks and steam-driven equilibria dominate: WGS reaction, steam methane reforming (reaction 6 on Table 4) and steam tar reforming all push the system toward higher H_2 and adjust the CH_4 balance (Mohammad Junaid and Khaled Ali, 2022). Consistent with these pathways, Cao et al. (2025) reported that in steam gasification at ~800 °C the H_2/CO ratio increases with temperature due to endothermic tar reforming and char–steam reactions. Under these conditions, methane concentrations remained moderate, around 3–5 vol% depending on the steam-to-biomass ratio, which is comparable to the 3–7.5 vol% CH_4 observed in this study. Moreover, Yang et al. (2019) showed in controlled fluidized-bed experiments that increasing the steam-to-biomass ratio raises H_2 while CO decreases, with CH_4 changing only slightly. This behavior is consistent with a competition between limited secondary methanation/hydrogasification ($CO/CO_2 + H_2 \rightleftharpoons CH_4$; $C + 2H_2 \rightleftharpoons CH_4$) and simultaneous steam reforming of CH_4 at 800 °C, which prevents excessive methane accumulation. When combined, these mechanisms can explain the higher H_2 and moderate CH_4 obtained under steam compared to air, and align with the broader fluidized-bed steam-gasification literature on temperature and steam-to-biomass ratio effects.

3.10. Thermochemical processes with nitrogen

For the experiments performed with nitrogen, the flow rates were selected solely based on fluidization test data. Tests were performed with the flow rates of 12, 15 and 18 NL·min^{-1}. The resulting gas formation profiles are shown in Fig. 4.

At 12 NL·min^{-1} of nitrogen, the production profiles of CO and H_2 followed similar trends, as did those of CH_4 and CO_2, suggesting the occurrence of the reverse methanation reaction (Equation 7, Table 4).

Since nitrogen contains no oxygen, oxidation reactions of the biomass carbon (which typically produce CO and CO_2) were suppressed. As a result, higher volumetric concentrations of H_2 — one of the most desirable gases — were achieved.

At nitrogen flow rate of 15 NL·min^{-1}, the same trend was observed, with formation of CO and CH_4 from 15 min of reaction. The process initially favored CO_2 and CO formation, followed by a progressive increase in H_2, reaching a peak of approximately 7 % near 40 min of reaction. The inverse behavior of the H_2 and CO_2 concentration curves again indicates the predominance of the reverse methanation reaction (Equation 7, Table 4), as it occurs for the condition with 12 NL·min^{-1}.

Under 18 NL·min^{-1} of nitrogen condition, H_2 became the

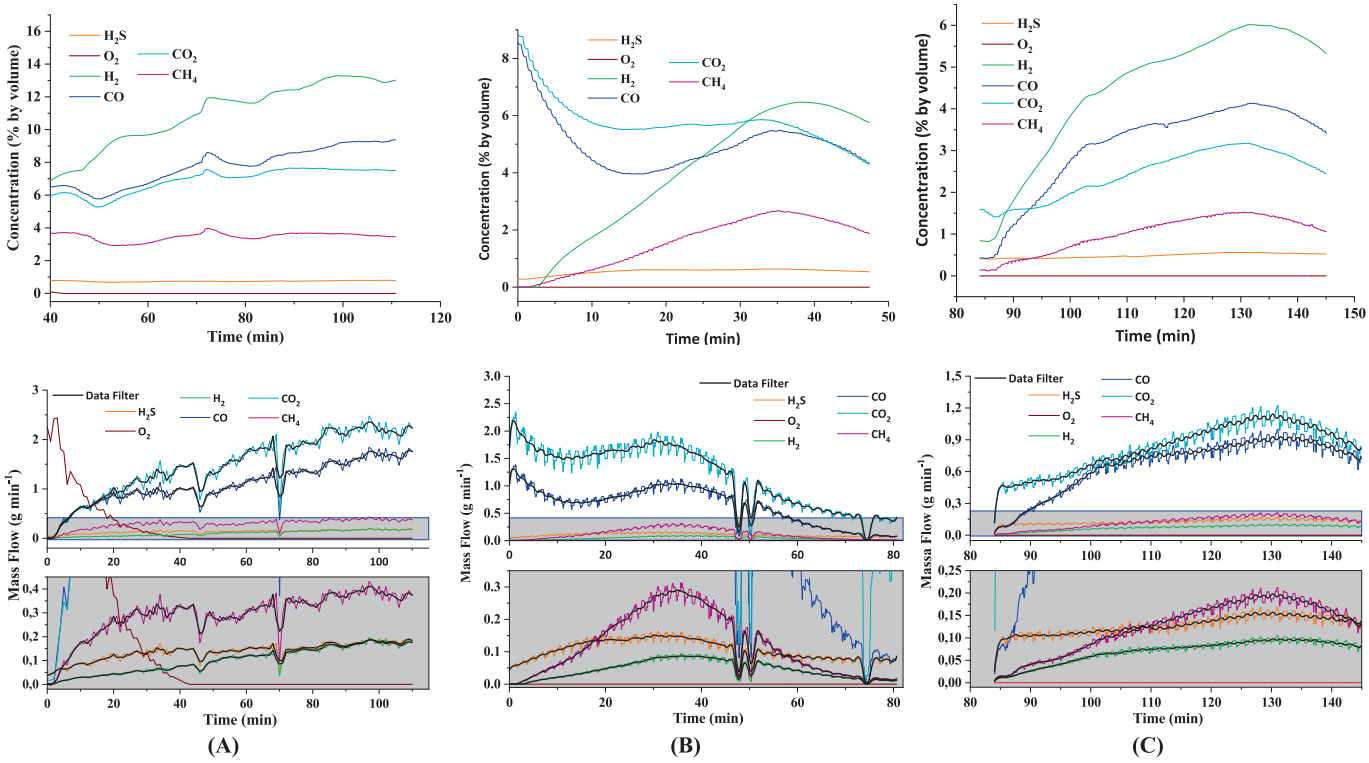

Fig. 4. Gas concentration and mass flow profiles during gasification of OPFEB with nitrogen at (A) 12 NL·min^{-1}, (B) 15 NL·min^{-1} and (C) 18 NL·min^{-1}.

predominant product, followed by CO and CO_2. Both H_2S and CH_4 were low, possibly due to the occurrence of the steam reforming reaction or partial oxidation of methane (Equations 7 or 8), since in both reactions CH_4 is consumed to produce CO and H_2.

3.11. *Performance of gasification agents: Relationship between produced gas mass and mass of biomass fed*

To evaluate the performance of the thermochemical processes with different fluidization agents (air, steam and nitrogen), an average yield of each gas was calculated using the mass ratio of produced gas to fed biomass (R_{gb}). This normalization enables a direct comparison of gasification performance across agents and operating conditions and helps account for process disturbances such as biomass feed fluctuations or temperature variations in the reactor bed. Fig. 5 presents the R_{gb} values for each gas under the different conditions tested.

In air gasification, gas yields increased as the equivalence ratio raised from 0.29 to 0.32 and from 0.32 to 0.36. Between 0.36 and 0.40, a slight decrease in CO_2 yield was observed, while yields of the other gases continued to increase. Finally, when raising ER from 0.40 to 0.43, there was an increase in CO and CO_2 conversions, but a small decrease in CH_4 and H_2 production, suggesting that ER = 0.40 may represent an optimal balance.

Under the two conditions evaluated with steam as the gasifying agent, increasing R_{sb} led to higher R_{gb} ratios for CO_2, H_2 and H_2S, while reducing CH_4 values; CO yield, however, remained essentially constant.

Under nitrogen atmospheres, increasing the flow rate from 12 to 15 NL·min^{-1} resulted in higher CO_2 and H_2S production, decreasing the R_{gb} ratio for CO, CH_4 and H_2, which is unfavorable for the process, since the latter are the main combustible gases of the generated gas mixture. Raising the flow to 18 NL·min^{-1} reversed this trend for most gases, except CH_4 (which remained nearly unchanged) and CO_2 (which decreased significantly).

Comparing the different agents, steam yielded the highest conversions to CH_4 and H_2, at 0.05 and 0.04 g of gas per gram of biomass, respectively. It was also observed that a high value was obtained for the ratio between the mass of biomass fed and the mass of CO produced (around 0.25 g CO generated per gram of OPFEB). However, the highest conversions of *in natura* biomass into CO were obtained in gasification using air, with a maximum of about 0.56 g of CO produced per gram of OPFEB at ER = 0.43.

The experimental results confirm the technical feasibility of OPEFB gasification and its potential for hydrogen-rich syngas production. However, it is also important to recognize some practical challenges that may affect large-scale implementation. Some challenges remain for the large-scale application of OPEFB gasification. Tar formation may occur due to the high volatile content of the biomass, potentially affecting downstream processes (Maitlo et al., 2022). The use of catalysts could enhance hydrogen yield and reduce tar but also introduce economic and operational limitations, such as deactivation and attrition (Jothiprakash et al., 2025). In addition, the relatively high potassium and chlorine contents in OPEFB ash may promote bed agglomeration and sintering, which could affect reactor stability (Kittivech and Fukuda, 2019). These aspects should be considered in future optimization studies.

4. Conclusions

The characterization of OPEFB demonstrated its potential as a feedstock for energy generation, thereby adding value to a residue from the palm oil production chain. The thermochemical processes using OPEFB under different gasifying agents – air, steam, and nitrogen – revealed distinct syngas compositions depending on the operating conditions. Air-based gasification resulted in a predominant production of CO and CO_2, with moderate H_2 and low CH_4 yields. In contrast, steam gasification led to a predominant production of H_2, reaching close to 50 % (v/v) and 0.05 g/g biomass, along with substantial CO and CO_2 and a modest increase in CH_4 relative to air. Nitrogen-based processes also produced high levels of H_2, followed by CO and CO_2, with CH_4 present in lower concentration. Among the nitrogen flow rates tested (12, 15, and 18 NL·min^{-1}), the 12 NL·min^{-1} condition yielded the highest

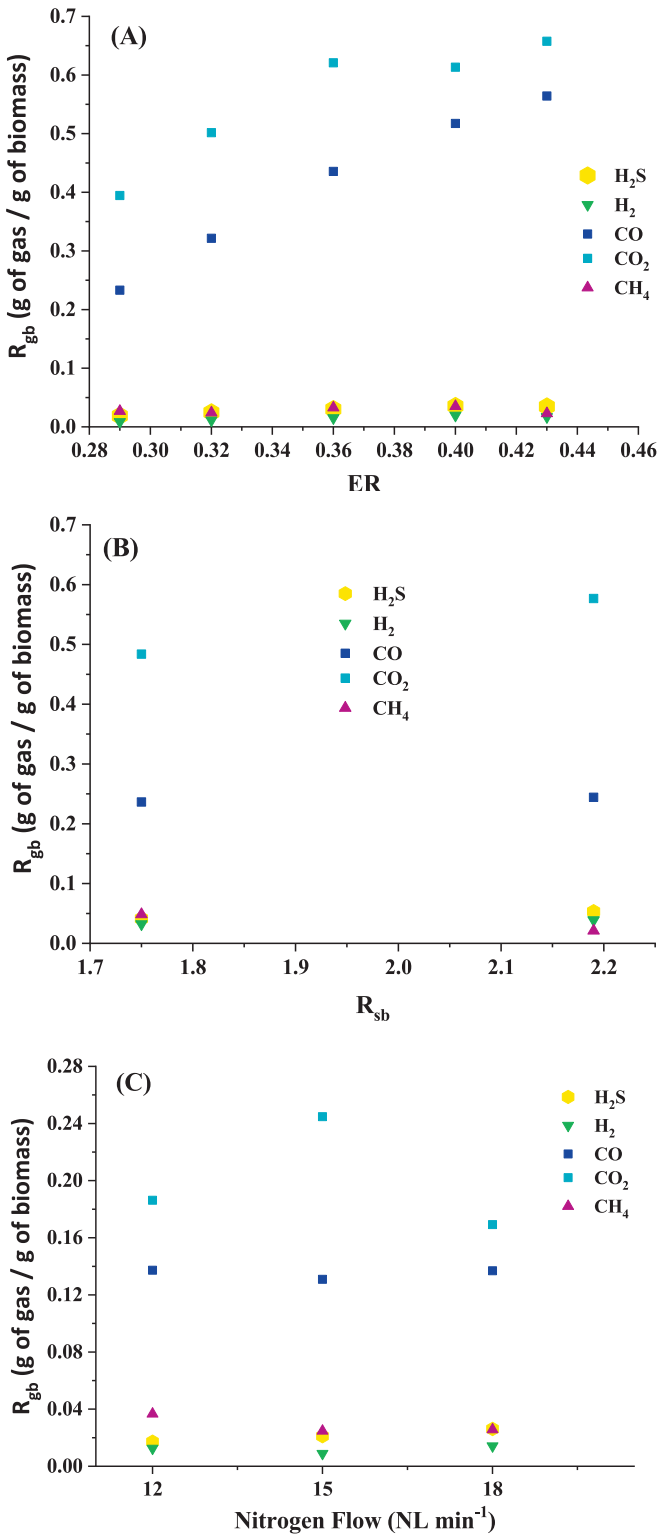

Fig. 5. Gas conversion profiles for OPFEB. (A) Air at ER 0.29, 0.32, 0.36, 0.40 and 0.43; (B) Steam with R_{sb} of 1.75 and 2.19, (C) Nitrogen Flow in 12, 15 and 18 NL.min^{-1}.

concentrations of the key gases of interest.

These yields are comparable to or higher than those reported for other lignocellulosic biomasses such as sugarcane bagasse and corn stover, underscoring the competitiveness of OPEFB for thermochemical conversion. Gasification is a well-established technology traditionally relying on coal, but the demonstration of OPEFB conversion in a pilot-scale fluidized bed reactor provides novel insights and confirms the technical feasibility of scaling agro-industrial residue valorization. This work highlights OPEFB as a promising resource for hydrogen-rich syngas production, advancing the scientific understanding of biomass gasification and supporting the integration of renewable feedstocks into sustainable energy and biorefinery systems.

CRediT authorship contribution statement

Amanda Assunção Rosa Silva: . **Gabriel Ferreira da Silva Brito:** . **Thainá Araruna:** Writing – review & editing, Writing – original draft, Visualization, Validation, Formal analysis. **Rossano Gambetta:** Writing – review & editing, Writing – original draft, Resources, Methodology, Funding acquisition, Conceptualization. **Fabricio Machado:** Writing – review & editing, Writing – original draft, Resources, Project administration, Methodology, Funding acquisition, Conceptualization.

Declaration of competing interest

The authors declare that they have no known competing financial interests or personal relationships that could have appeared to influence the work reported in this paper.

Acknowledgments

This work was partially supported by Conselho Nacional de Desenvolvimento Científico e Tecnológico (CNPq) – Process 310829/2021-6, Coordenação de Aperfeiçoamento de Pessoal de Nível Superior (CAPES) – Finance Code 001, and Financiadora de Estudos e Projetos (FINEP) – grant n° 01.13.0315.02. The authors thank Fundação de Apoio à Pesquisa do Distrito Federal (FAPDF), Embrapa Agroenergia for providing scholarships and research support.

Appendix A. Supplementary data

Supplementary data to this article can be found online at https://doi.org/10.1016/j.biortech.2025.133404.

Data availability

Data will be made available on request.

References

Ahmad, N.N., Ahmad, A.A., Khasri, A., 2023. Effective removal of methylene blue from aqueous solution by adsorption onto gasification char: Isotherm, kinetic and thermodynamics studies. Desalin. Water Treat. 285, 264–273. https://doi.org/10.5004/dwt.2023.29274.

Al Zubi, M.A., Areche, F.O., Morales Alberto, M.N., Cotrina Cabello, G.G., Gomez, A.S., Legua Cardenas, J.A., Zevallos, M.L., Lijarza Llanos, Y.Y., Morsy, K., Quincho Astete, J.A., Castañeda Chirre, E.T., Choque Rivera, T.J., Aguilar, S.V., Sánchez Araujo, V.G., Quispe-Vidalon, J., 2023. Conversion of lignocellulose biomass to bioenergy through nanobiotechnology. J. Sustain. Develop. Energy, Water Environ. Syst. 11 (2), 1100442. https://doi.org/10.13044/j.sdewes.d11.0442.

Al-Muraisy, S.A.A., Chuayboon, S., Soares, L.A., Buijnsters, J.G., Ismail, S.B., Abanades, S., van Lier, J.B., Lindeboom, R.E.F., 2025. Carbon capture through solar-driven CO2 gasification of oil palm empty fruit bunch to produce syngas and biochar. Energy 323, 135805. https://doi.org/10.1016/j.energy.2025.135805.

Alauddin, Z.A.B.Z., Lahijani, P., Mohammadi, M., Mohamed, A.R., 2010. Gasification of lignocellulosic biomass in fluidized beds for renewable energy development: A review. Renew. Sustain. Energy Rev. 14 (9), 2852–2862. https://doi.org/10.1016/j.rser.2010.07.026.

Ang, T.-Z., Salem, M., Kamarol, M., Das, H.S., Nazari, M.A., Prabaharan, N., 2022. A comprehensive study of renewable energy sources: Classifications, challenges and suggestions. Energ. Strat. Rev. 43, 100939. https://doi.org/10.1016/j.esr.2022.100939.

Asadpour, R., Yavari, S., Kamyab, H., Ashokkumar, V., Chelliapan, S., Yuzir, A., 2021. Study of oil sorption behaviour of esterified oil palm empty fruit bunch (OPEFB) fibre and its kinetics and isotherm studies. Environ. Technol. Innovation 22, 101397. https://doi.org/10.1016/j.eti.2021.101397.

Bilgili, F., Koçak, E., Bulut, Ü., Kuşkaya, S., 2017. Can biomass energy be an efficient policy tool for sustainable development? Renew. Sustain. Energy Rev. 71, 830–845. https://doi.org/10.1016/j.rser.2016.12.109.

Cao, Y., Bai, Y., Du, J., 2025. CaO-based sorption-enhanced steam gasification of biomass for high purity H2 production: A modeling approach. Biomass Convers. Biorefin. 15 (9), 13817–13829. https://doi.org/10.1007/s13399-024-06119-7.

Chan, Y.H., Syed Abdul Rahman, S.N.F., Lahuri, H.M., Khalid, A., 2021. Recent progress on CO-rich syngas production via CO2 gasification of various wastes: A critical review on efficiency, challenges and outlook. Environ. Pollut. 278, 116843. https://doi.org/10.1016/j.envpol.2021.116843.

Cherwoo, L., Gupta, I., Flora, G., Verma, R., Kapil, M., Arya, S.K., Ravindran, B., Khoo, K. S., Bhatia, S.K., Chang, S.W., Ngamcharussrivichai, C., Ashokkumar, V., 2023. Biofuels an alternative to traditional fossil fuels: A comprehensive review. Sustain. Energy Technol. Assess. 60, 103503. https://doi.org/10.1016/j.seta.2023.103503.

Chuaboon, L., Saengsen, C., Sookbampen, O., Yang, E., Shukor, H., Chisti, Y., Rongwong, W., 2024. Enhanced production of levulinic acid from oil palm empty fruit bunch. Waste Biomass Valorization 15 (10), 5771–5784. https://doi.org/10.1007/s12649-024-02500-9.

Cortez, L.A.B., Lora, E.E.S., Gómez, E.O., 2008. Biomassa para energia. Campinas, SP.

David, E., 2013. Valorization of residual biomass by thermochemical processing. J. Anal. Appl. Pyrol. 104, 260–268. https://doi.org/10.1016/j.jaap.2013.07.007.

Fernandes, U., Costa, M., 2010. Potential of biomass residues for energy production and utilization in a region of Portugal. Biomass Bioenergy 34 (5), 661–666. https://doi.org/10.1016/j.biombioe.2010.01.009.

Figueroa, J.E.J., Ardila, Y.C., Filho, R.M., Maciel, M.R.W., 2014. Fluidized bed reactor for gasification of sugarcane bagasse: Distribution of syngas, bio-tar and char. Chem. Eng. Trans. 37, 229–234. https://doi.org/10.3303/CET1437039.

Fremaux, S., Beheshti, S.-M., Ghassemi, H., Shahsavan-Markadeh, R., 2015. An experimental study on hydrogen-rich gas production via steam gasification of biomass in a research-scale fluidized bed. Energ. Conver. Manage. 91, 427–432. https://doi.org/10.1016/j.enconman.2014.12.048.

Fu, Z., Aghdam, N.C., Nekoeian, S., He, J., Cheng, L., Liu, S., Zhang, L., Chao, J., Wei, X., Wang, R., Nagda, B., Zhang, Y., Ma, Z., Ellis, N., Bi, X., Smith, K., Lim, J., Legros, R., Duo, W., 2025. Hot syngas cleanup for pilot two-stage fluidized bed steam-oxygen biomass gasification plant. Bioresour. Technol. 418, 131876. https://doi.org/10.1016/j.biortech.2024.131876.

Gao, Y., Wang, M., Raheem, A., Wang, F., Wei, J., Xu, D., Song, X., Bao, W., Huang, A., Zhang, S., Zhang, H., 2023. Syngas production from biomass gasification: Influences of feedstock properties, reactor type, and reaction parameters. ACS Omega 8 (35), 31620–31631. https://doi.org/10.1021/acsomega.3c03050.

Gayen, D., Chatterjee, R., Roy, S., 2023. A review on environmental impacts of renewable energy for sustainable development. Int. J. Environ. Sci. Technol. 21 (5), 5285–5310. https://doi.org/10.1007/s13762-023-05380-z.

Gómez-Barea, A., Leckner, B., 2010. Modeling of biomass gasification in fluidized bed. Prog. Energy Combust. Sci. 36 (4), 444–509. https://doi.org/10.1016/j.pecs.2009.12.002.

Hendrasetiafitri, C., Sung, Y.J., Kim, D.-S., 2022. Effects of pretreatments on the chemical composition and thermal conversion of oil palm empty fruit bunch. BioResources 17 (2), 2727–2742. https://doi.org/10.15376/biores.17.2.2727-2742.

Hidalgo, D., Urueña, A., Martín-Marroquín, J.M., Díez, D., 2025. Integrated approach for biomass conversion using thermochemical routes with anaerobic digestion and syngas fermentation. Sustainability 17 (8), 3615. https://doi.org/10.3390/su17083615.

Hossain, M.A., Jewaratnam, J., Ganesan, P., 2016. Prospect of hydrogen production from oil palm biomass by thermochemical process – A review. Int. J. Hydrogen Energy 41 (38), 16637–16655. https://doi.org/10.1016/j.ijhydene.2016.07.104.

Ismael, M.A., El-Adawy, M., Farooqi, A.S., Hamdy, M., Shahid, M.Z., Elserfy, Z., Nemitallah, M.A., 2025. Sustainable aviation fuel: Operational challenges, techno-economics, and life cycle analysis. Energy Fuels 39 (29), 13848–13878. https://doi.org/10.1021/acs.energyfuels.5c01606.

Jamil, F., Inayat, A., Hussain, M., Akhter, P., Abideen, Z., Ghenai, C., Shanableh, A., Abdellatief, T.M.M., 2024. Valorization of waste biomass to biofuels for power production and transportation in optimized way: A comprehensive review. Adv. Energy Sustain. Res. 5 (10), 2400104. https://doi.org/10.1002/aesr.202400104.

Jenkins, B.M., Baxter, L.L., Miles Jr., T.R., Miles, T.R., 1998. Combustion properties of biomass. Fuel Process. Technol. 54 (1–3), 17–46. https://doi.org/10.1016/S0378-3820(97)00059-3.

Jothiprakash, G., Balasubramaniam, P., Sundaram, S., Ramesh, D., 2025. Catalytic biomass gasification for syngas production: Recent progress in tar reduction and future perspectives. Biomass 5 (3), 37. https://doi.org/10.3390/biomass5030037.

Kalinci, Y., Hepbasli, A., Dincer, I., 2011. Comparative exergetic performance analysis of hydrogen production from oil palm wastes and some other biomasses. Int. J. Hydrogen Energy 36 (17), 11399–11407. https://doi.org/10.1016/j.ijhydene.2011.04.025.

Kelly-Yong, T.L., Lee, K.T., Mohamed, A.R., Bhatia, S., 2007. Potential of hydrogen from oil palm biomass as a source of renewable energy worldwide. Energy Policy 35 (11), 5692–5701. https://doi.org/10.1016/j.enpol.2007.06.017.

Khan, A.A., de Jong, W., Jansens, P.J., Spliethoff, H., 2009. Biomass combustion in fluidized bed boilers: Potential problems and remedies. Fuel Process. Technol. 90 (1), 21–50. https://doi.org/10.1016/j.fuproc.2008.07.012.

Kittivech, T., Fukuda, S., 2019. Effect of bed material on bed agglomeration for palm empty fruit bunch (efb) gasification in a bubbling fluidised bed system. Energies 12 (22), 4336. https://doi.org/10.3390/en12224336.

Klüh, D., Anetjärvi, E., Melin, K., Vakkilainen, E., 2024. Comparative techno-economic assessment of methanol production via directly and indirectly electrified biomass gasification routes. Energ. Conver. Manage. 314, 118649. https://doi.org/10.1016/j.enconman.2024.118649.

Kumar, A.K., Sharma, S., 2017. Recent updates on different methods of pretreatment of lignocellulosic feedstocks: A review. Bioresources Bioprocess. 4 (1), 7. https://doi.org/10.1186/s40643-017-0137-9.

Kuo, J.-H., Lin, C.-L., Ho, C.-Y., 2022. Effect of fluidization/gasification parameters on hydrogen generation in syngas during fluidized-bed gasification process. Int. J. Hydrogen Energy 47 (96), 40656–40663. https://doi.org/10.1016/j.ijhydene.2021.03.070.

Kurnia, J.C., Jangam, S.V., Akhtar, S., Sasmito, A.P., Mujumdar, A.S., 2016. Advances in biofuel production from oil palm and palm oil processing wastes: A review. Biofuel Res. J. 3 (1), 332–346. https://doi.org/10.18331/brj2016.3.1.3.

Lahijani, P., Zainal, Z.A., 2011. Gasification of palm empty fruit bunch in a bubbling fluidized bed: A performance and agglomeration study. Bioresour. Technol. 102 (2), 2068–2076. https://doi.org/10.1016/j.biortech.2010.09.101.

Maglinao, A.L., Capareda, S.C., Nam, H., 2015. Fluidized bed gasification of high tonnage sorghum, cotton gin trash and beef cattle manure: Evaluation of synthesis gas production. Energ. Conver. Manage. 105, 578–587. https://doi.org/10.1016/j.enconman.2015.08.005.

Maitlo, G., Ali, I., Mangi, K.H., Ali, S., Maitlo, H.A., Unar, I.N., Pirzada, A.M., 2022. Thermochemical conversion of biomass for syngas production: Current status and future trends. Sustainability 14 (5), 2596. https://doi.org/10.3390/su14052596.

Mankasem, J., Prasertcharoensuk, P., Phan, A.N., 2024. Intensification of two-stage biomass gasification for hydrogen production. Int. J. Hydrogen Energy 49, 189–202. https://doi.org/10.1016/j.ijhydene.2023.07.212.

Martínez, J.D., Mahkamov, K., Andrade, R.V., Silva Lora, E.E., 2012. Syngas production in downdraft biomass gasifiers and its application using internal combustion engines. Renew. Energy 38 (1), 1–9. https://doi.org/10.1016/j.renene.2011.07.035.

Méndez-Durazno, C., Robles Carrillo, N.M., Ramírez, V., Chico-Proano, A., Debut, A., Espinoza-Montero, P.J., 2024. Bioenergy potential from Ecuadorian lignocellulosic biomass: Physicochemical characterization, thermal analysis and pyrolysis kinetics. Biomass Bioenergy 190, 107381. https://doi.org/10.1016/j.biombioe.2024.107381.

Miccio, F., Raganati, F., Ammendola, P., Okasha, F., Miccio, M., 2021. Fluidized bed combustion and gasification of fossil and renewable slurry fuels. Energies 14 (22), 7766. https://doi.org/10.3390/en14227766.

Mignogna, D., Szabó, M., Ceci, P., Avino, P., 2024. Biomass energy and biofuels: perspective, potentials, and challenges in the energy transition. Sustainability 16 (16), 7036. https://doi.org/10.3390/su16167036.

Mohammad Junaid, K., Khaled Ali, A.-A., 2022. Steam gasification of biomass for hydrogen production – A review and outlook. J. Adv. Res. Fluid Mech. Therm. Sci. 98 (2), 175–204. https://doi.org/10.37934/arfmts.98.2.175204.

Mohammed, M.A.A., Salmiaton, A., Wan Azlina, W.A.K.G., Mohammad Amran, M.S., A., Fakhru'l-Razi, 2011. Air gasification of empty fruit bunch for hydrogen-rich gas production in a fluidized-bed reactor. Energ. Conver. Manage. 52 (2), 1555–1561. https://doi.org/10.1016/j.enconman.2010.10.023.

Molino, A., Chianese, S., Musmarra, D., 2016. Biomass gasification technology: The state of the art overview. J. Energy Chem. 25 (1), 10–25. https://doi.org/10.1016/j.jechem.2015.11.005.

Musinguzi, W.B., Okure, M.A.E., Sebbit, A., Løvås, T., da Silva, I., 2014. Thermodynamic modeling of allothermal steam gasification in a downdraft fixed-bed gasifier. Adv. Mat. Res. 875–877, 1782–1793. https://doi.org/10.4028/www.scientific.net/AMR.875-877.1782.

Mustafa, A., Faisal, S., Singh, J., Rezki, B., Kumar, K., Moholkar, V.S., Kutlu, O., Aboulmagd, A., Khamees Thabet, H., El-Bahy, Z.M., Der, O., Ussemane Mussagy, C., di Bitonto, L., Ahmad, M., Pastore, C., 2024. Converting lignocellulosic biomass into valuable end products for decentralized energy solutions: A comprehensive overview. Sustain. Energy Technol. Assess. 72, 104065. https://doi.org/10.1016/j.seta.2024.104065.

Nyakuma, B.B., Wong, S.L., Oladokun, O., Bello, A.A., Hambali, H.U., Abdullah, T.A.T., Wong, K.Y., 2020. Review of the fuel properties, characterisation techniques, and pre-treatment technologies for oil palm empty fruit bunches. Biomass Convers. Biorefin. 13 (1), 471–497. https://doi.org/10.1007/s13399-020-01133-x.

Obada, D.O., Kekung, M.O., Levonyan, T., Norval, G.W., 2023. Palm oil mill derived empty palm fruit bunches as a feed stock for renewable energy applications in Nigeria: A review. Bioresour. Technol. Rep. 24, 101666. https://doi.org/10.1016/j.biteb.2023.101666.

Pacheco, M., Moura, P., Silva, C., 2023. A systematic review of syngas bioconversion to value-added products from 2012 to 2022. Energies 16 (7), 3241. https://doi.org/10.3390/en16073241.

Padzil, F.N.M., Lee, S.H., Ainun, Z.M.A., Lee, C.H., Abdullah, L.C., 2020. Potential of oil palm empty fruit bunch resources in nanocellulose hydrogel production for versatile applications: A review. Materials 13 (5), 1245. https://doi.org/10.3390/ma13051245.

Pedroso, D.T., Machin, E.B., Cabrera-Barjas, G., Flores, M., Urra, H.G., de Carvalho, F.S., Santos, M.I.S.D., Machín, A.B., Canettieri, E.V., Pérez, N.P., Teixeira Lacava, P., Ribeiro dos Santos, L., de Carvalho, Andrade, Júnior, J., 2021. sugarcane bagasse torrefaction for fluidized bed gasification. Appl. Sci. 11 (13), 6105. https://doi.org/10.3390/app11136105.

Pfeifer, C., Koppatz, S., Hofbauer, H., 2011. Steam gasification of various feedstocks at a dual fluidised bed gasifier: Impacts of operation conditions and bed materials. Biomass Convers. Biorefinery 1 (1), 39–53. https://doi.org/10.1007/s13399-011-0007-1.

Razm, S., Brahimi, N., Hammami, R., Dolgui, A., 2023. A production planning model for biorefineries with biomass perishability and biofuel transformation. Int. J. Prod. Econ. 258, 108773. https://doi.org/10.1016/j.ijpe.2023.108773.

Ruiz, J.A., Juárez, M.C., Morales, M.P., Muñoz, P., Mendívil, M.A., 2013. Biomass gasification for electricity generation: Review of current technology barriers. Renew. Sustain. Energy Rev. 18, 174–183. https://doi.org/10.1016/j.rser.2012.10.021.

Saidur, R., Abdelaziz, E.A., Demirbas, A., Hossain, M.S., Mekhilef, S., 2011. A review on biomass as a fuel for boilers. Renew. Sustain. Energy Rev. 15 (5), 2262–2289. https://doi.org/10.1016/j.rser.2011.02.015.

Sansaniwal, S.K., Pal, K., Rosen, M.A., Tyagi, S.K., 2017. Recent advances in the development of biomass gasification technology: A comprehensive review. Renew. Sustain. Energy Rev. 72, 363–384. https://doi.org/10.1016/j.rser.2017.01.038.

Santana, H.E.P., Jesus, M., Santos, J., Rodrigues, A.C., Pires, P., Ruzene, D.S., Silva, I.P., Silva, D.P., 2025. Lignocellulosic biomass gasification: Perspectives, challenges, and methods for tar elimination. Sustainability 17 (5), 1888. https://doi.org/10.3390/su17051888.

Santos, R.G.D., Alencar, A.C., 2020. Biomass-derived syngas production via gasification process and its catalytic conversion into fuels by Fischer Tropsch synthesis: A review. Int. J. Hydrogen Energy 45 (36), 18114–18132. https://doi.org/10.1016/j.ijhydene.2019.07.133.

Santos, S.M., Assis, A.C., Gomes, L., Nobre, C., Brito, P., 2022. Waste gasification technologies: A brief overview. Waste 1 (1), 140–165. https://doi.org/10.3390/waste1010011.

Sarker, S., Bimbela, F., Sánchez, J.L., Nielsen, H.K., 2015. Characterization and pilot scale fluidized bed gasification of herbaceous biomass: A case study on alfalfa pellets. EnergyConvers. Manage. 91, 451–458. https://doi.org/10.1016/j.enconman.2014.12.034.

Shahzad, H.M.A., Asim, Z., Khan, S.J., Almomani, F., Mahmoud, K.A., Mustafa, M.R.U., Rasool, K., 2024. Thermochemical and biochemical conversion of agricultural waste for bioenergy production: an updated review. Discover Environ. 2 (1), 134. https://doi.org/10.1007/s44274-024-00171-w.

Sher, F., Hameed, S., Smječanin Omerbegović, N., Chupin, A., Ul Hai, I., Wang, B., Heng Teoh, Y., Joka Yildiz, M., 2025. Cutting-edge biomass gasification technologies for renewable energy generation and achieving net zero emissions. Energ. Conver. Manage. 323, 119213. https://doi.org/10.1016/j.enconman.2024.119213.

Siddiqui, M.Z., Sheraz, M., Toor, U.A., Anus, A., Mahmood, A., Haseeb, M., Ibrahim, M., Khoo, K.S., Devadas, V.V., Mubashir, M., Ullah, S., Show, P.L., 2022. Recent approaches on the optimization of biomass gasification process parameters for product H2 and syngas ratio: A review. Environ. Dev. Sustain. https://doi.org/10.1007/s10668-022-02279-6.

Sidek, F.N., Saleh, S., Samad, N.A.F.A., 2021. Gasification performance and tar generation comparison from fluidized bed gasification of raw and torrefied empty fruit bunch. IOP Conf. Ser.: Mater. Sci. Eng. 1092 (1), 012061. https://doi.org/10.1088/1757-899x/1092/1/012061.

Singh, S., Nara, R., Yadav, M., Sharma, C., Agrawal, S., Kumar, A., 2025. Oil palm biomass: A potential feedstock for lignocellulolytic enzymes and biofuels production. Environ. Sci. Pollut. Res. 32 (19), 11791–11814. https://doi.org/10.1007/s11356-025-36379-3.

Strielkowski, W., Civín, L., Tarkhanova, E., Tvaronavičienė, M., Petrenko, Y., 2021. Renewable energy in the sustainable development of electrical power sector: A review. Energies 14 (24), 8240. https://doi.org/10.3390/en14248240.

Sukiran, M., Abu Bakar, N.K., Chin, C., 2009. Optimization of pyrolysis of oil palm empty fruit bunches. J. Oil Palm Res. 21 (2), 653–658.

Tanimu, I.M., Hernandez, E., Bachmann, R.T., 2025. Biogas potential of oil palm empty fruit bunch and lignocellulosic insoluble fibre components via the syringe bioreactor method. Fuel 385, 134087. https://doi.org/10.1016/j.fuel.2024.134087.

Umar, H.A., Sulaiman, S.A., Meor Said, M.A., Gungor, A., Shahbaz, M., Inayat, M., Ahmad, R.K., 2021. Assessing the implementation levels of oil palm waste conversion methods in Malaysia and the challenges of commercialisation: Towards sustainable energy production. Biomass Bioenergy 151, 106179. https://doi.org/10.1016/j.biombioe.2021.106179.

Vassilev, S.V., Baxter, D., Andersen, L.K., Vassileva, C.G., Morgan, T.J., 2012. An overview of the organic and inorganic phase composition of biomass. Fuel 94, 1–33. https://doi.org/10.1016/j.fuel.2011.09.030.

Vassilev, S.V., Vassileva, C.G., Vassilev, V.S., 2015. Advantages and disadvantages of composition and properties of biomass in comparison with coal: An overview. Fuel 158, 330–350. https://doi.org/10.1016/j.fuel.2015.05.050.

Yana, S., Nizar, M., Irhamni, M., D., 2022. Biomass waste as a renewable energy in developing bio-based economies in Indonesia: A review. Renew. Sustain. Energy Rev. 160, 112268. https://doi.org/10.1016/j.rser.2022.112268.

Yang, H.M., Liu, J.G., Zhang, H., Han, X.X., Jiang, X.M., 2019. Experimental research for biomass steam gasification in a fluidized bed. Energy Sources, Part A: Recovery, Utilization, Environ. Effects 41 (16), 1993–2006. https://doi.org/10.1080/15567036.2018.1549128.